Location of Mg Cations in Mordenite Zeolite Studied by IR Spectroscopy and Density Functional Theory Simulations with a CO Adsorption Probe

ARTICLE *in* THE JOURNAL OF PHYSICAL CHEMISTRY A · MARCH 2008

Impact Factor: 2.69 · DOI: 10.1021/jp709635f · Source: PubMed

Location of Mg Cations in Mordenite Zeolite Studied by IR Spectroscopy and Density Functional Theory Simulations with a CO Adsorption Probe

Keju Sun,[‡,§] Weiguang Su,[‡,§] Fengtao Fan,[‡,§] Zhaochi Feng,[‡] Tonek A. P. J. Jansen,[#] Rutger A. van Santen,[*,#] and Can Li[*,‡]

State Key Laboratory of Catalysis, Dalian Institute of Chemical Physics, Chinese Academy of Sciences, 457 Zhongshan Road, Dalian 116023, China, Graduate University of Chinese Academy of Sciences, Beijing 100049, China, and Department of Chemical Engineering and Chemistry Molecular Heterogeneous Catalysis, Eindhoven University of Technology, P.O. Box 513, 5600 MB, Eindhoven, The Netherlands

Received: October 2, 2007; In Final Form: November 22, 2007

The location of Mg cations in the channel of mordenite zeolite was studied using a combination of DFT simulations and IR spectroscopy of adsorbed CO. The calculated adsorption energies and frequencies of CO on Mg cations are in good agreement with the results from the IR spectra of adsorbed CO. It is found that the Mg cations can occupy the sites A, C, D and E in mordenite and the distribution of the Mg cations in these sites follows the priority order, site C > site A > site D and site E.

Introduction

Zeolites are a class of very useful materials in catalysis and gas adsorption because of their unique properties particularly derived from ion exchange.[1−7] The exchanged ions in zeolites play a decisive role in their properites.[8] However, design, synthesis and efficient utilization of zeolites with exchanged ions require a thorough understanding of the location of the exchanged ions and the properties of the exchanged ions such as adsorption, acidity−basicity and catalysis.

Several methods were used to study the siting of exchanged ions in zeolites. Single-crystal X-ray diffraction (XRD) is a useful technique for zeolite characterization.[9] However, identification of metal cation sites in high-silica zeolites (Si/Al > 6) by employing XRD encounters difficulties because of the low cation concentration in zeolites. In addition, the preparation of single crystals of zeolites for XRD measurement is difficult for high-silica zeolites.[8] Some other methods such as EXAFS, laser-induced emission spectroscopy and TEM could supply some indirect information but are still limited to the study on the location of exchanged ions.[8] Therefore, to locate the position of exchanged cations in zeolites remains a challenge.

Although IR spectra of adsorbed probe molecules on metal ions may not directly define the local geometry of exchanged ions in zeolites, they can differentiate the behaviors of metal ions at different sites and can be used to determine their relative population in zeolites.[10−12] The intensities of vibrational bands of adsorbed CO at low temperatures can in principle provide the approximate distribution of the active site at different sites. Furthermore, the variation of IR band intensity of adsorbed CO with the temperature can give useful information about the interaction energy of CO molecules with adsorption sites in zeolites. Interaction of the CO molecule with the cation has a net positive charge that shifts the C−O stretching frequency from that of the free molecule (2143 cm^{-1}) to higher values.[13] The magnitude of this blue shift could be a measure of the corresponding electrostatic field strength surrounding the cation.

The important information such as IR frequencies and binding energies of adsorbed CO to metal cations at different sites can be obtained by IR spectroscopy; however the local geometry of the cation, *i.e.*, its cationic site, in zeolites is difficult to directly determine. DFT simulations could provide the vibrational frequencies and the binding energies of adsorbed CO with the metal ions and the local geometries of the ions.[14−17] Thus, in principle, the siting of metal ions in zeolite could be resolved on the basis of the vibrational frequencies and binding energies deduced from IR spectroscopy and DFT calculations.

In this work, CO adsorption on Mg cation exchanged mordenite (MOR) was investigated by combining IR sepectroscopy and DFT simulations. The location and concentration of the Mg cations in the different sites of mordenite zeolite have been identified, and the adsorption energies and IR frequencies of adsorbed CO on Mg^{2+} exchanged mordenite have also been studied.

Computational and Experimental Methods

Computational Details. Two different approaches in DFT calucations were chosen: the cluster approach and the periodical approach. Both approaches have already been used to study the adsorption to zeolitic cations.[14−17] The cluster approach is a suitable method to accurately predict the local properties such as equilibrium geometries and vibrational frequencies, rather than properties as the binding energies, that depend on substrate electronic properties that can be more precisely predicted by periodical approaches.[18−24] Therefore, in this article, the energies were calculated through periodical approach and the frequencies were mainly predicted using cluster approach.

Mordenite zeolite is selected as a model zeolite in this work for following reasons. First, mordenite is one of the most common zeolites. It has been widely used as a catalyst for the cracking and isomerization of hydrocarbons, dewaxing of heavy petroleum fractions and methanol conversion to

* To whom correspondence should be addressed. C.L.: tel, 86-411-84379070; fax, 86-411-84694447; e-mail, canli@dicp.ac.cn; homepage, http://www.canli.dicp.ac.cn. R.A.v.S.: tel, 31-40-2473082; fax, 31-40-2455054; e-mail, R.A.v.Santen@tue.nl.

‡ Dalian Institute of Chemical Physics, Chinese Academy of Sciences.

§ Graduate University of Chinese Academy of Sciences.

Eindhoven University of Technology.

10.1021/jp709635f CCC: $40.75
Published on Web 01/24/2008

SCHEME 1: Structure of Mordenite with Different Sites Available for Ion Exchange[a]

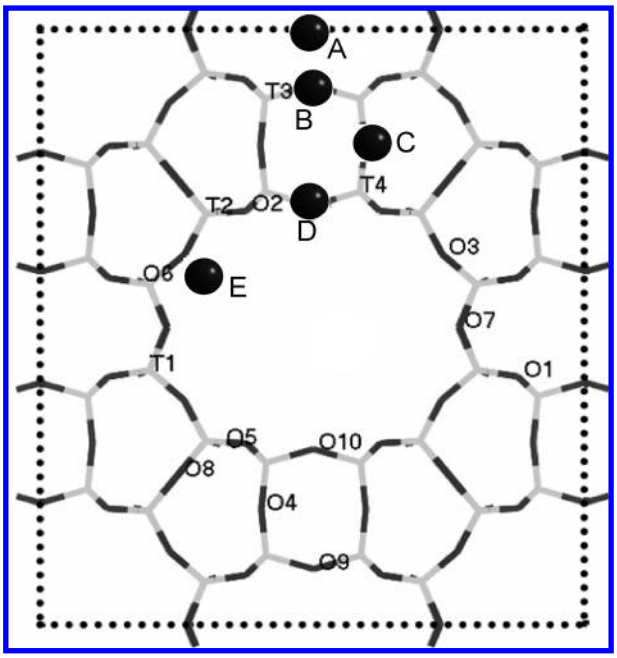

[a] A, B, C, D and E represent the five possible positions of exchanged cations.

hydrocarbons.[3,4,25−27] Second, mordenite with its small unit cell (18.1 Å × 20.5 Å × 7.5 Å) is not highly computational demonstrating. Finally, three types of cavities and five possible exchanged sites are present in mordenite (see Scheme 1), and the different adsorption sites in mordenite can be compared with each other.

Mg cation was selected to model the adsorption site in a zeolite. Its small ionic radius (0.66 Å) and high positive charge (+2) may be expected to lead to high electrostatic field. The strength of this electrostatic field is linearly related to the frequency shifts of adsorbed CO. One may expect an interaction that provides such a large blue shift to distinguish CO adsorbed on Mg cation located at different sites. CO adsorbed on a Mg cation exchanged zeolites at low temperature mainly forms linear monocarbonyls due to the small ionic radius of Mg^{2+};[28] therefore, only monocarbonyls are considered, which considerably simplifies the model.

Periodical *ab initio* calculations have been performed using the Vienna *Ab initio* Simulation Package (VASP).[29] The total energy is calculated by solving the Kohn−Sham equations, using the exchange-correlation functional proposed by Perdew and Zunger.[30] Results are corrected for nonlocality in the generalized gradient approximation with the Perdew Wang 91 functional.[31] VASP uses plane waves, ultrasoft pseudopotentials provided by Kresse and Hafner,[32] allowing a significant reduction of the number of plane waves. For the calculations, a cutoff of 400 eV and a Brillouin-zone sampling restricted to the Γ-point have been used. The augmentation charges were expanded to 900 eV.

The geometry of the unit cell of mordenite has previously been defined using VASP by Demuth et al.[33] To avoid artificial interactions of the molecules, the minimal unit cell of mordenite was doubled in the main channel direction. Structural relaxation, energies and frequencies of all the compounds have been done by employing a quasi-Newton algorithm based on the minimization of analytical forces. Convergence has been considered to be achieved when forces on the unit cell atoms are less than 0.05 eV $Å^{-1}$.

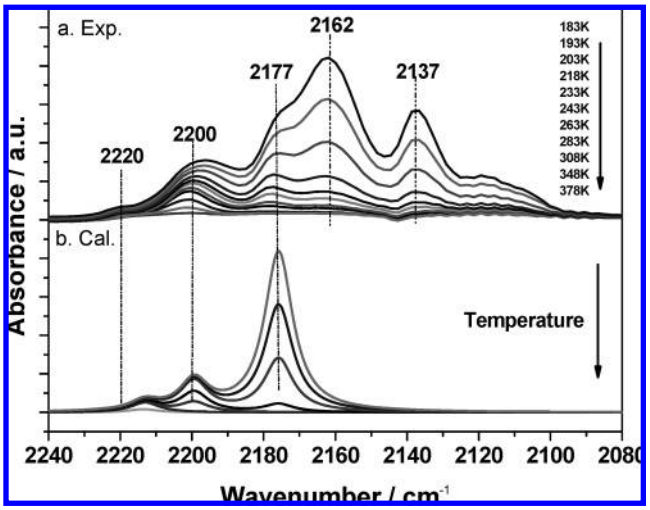

Figure 1. (a) IR spectra of adsorbed CO on MgK/mordenite at temperatures 183−378 K. (b) Calculated IR spectra of adsorbed CO on Mg/mordenite with the increasing temperature by DFT simulations.

Three types of cavities are present in mordenite: (i) a main channel circumscribed by ellipsoidal twelve-membered rings, measuring 7 × 6.5 Å, (ii) a side channel with strongly compressed eight-membered rings parallel to the main channel, measuring 5.7 × 2.6 Å and (iii) a side pocket circumscribed by another set of compressed eight-membered rings connecting the main channels and the side channels perpendicular to main channel, measuring 3.4 × 4.8 Å.[34] There are five possible positions of exchanged cations (A through E in Scheme 1) in the mordenite zeolite.[8,35] Site A is a twisted eight-ring located in the elliptical eight-ring channels of mordenite. Site B is in the circular eight-rings, situated in the walls of the elliptical eight-ring channel. Site C is located in the eight-ring channel of the zeolite, which is composed of a nonplanar six-ring in two bent five-rings. Site D is in the circular eight-rings, situated in the walls of the large twelve-ring channel, and site E is the six-ring in the twelve-member ring channel.

In accordance with Loewenstein's rule[36] and Takaishi's additional rule[37,38] for aluminum distribution in mordenite, there are many possibilities for placing two aluminums in the position near site A. Only one structure (Period-Mor-A) with two aluminums referenced to the literature[39] was selected (the position of aluminum atoms is shown in Scheme 2a). To simulate the Mg cation in site B, we calculated two structures: one (Period-Mor-B1) is that the silicon atoms in T3 and T3 sites are replaced by aluminum atoms, the other (Period-Mor-B2) is that the silicon atoms in T3 and T1 sites are substituted. Considering the symmetry, only one structure (Period-Mor-C) exists in site C (see Scheme 2b for the position of aluminum atoms). Similar to site B, two structures were chosen for site D: one (Period-Mor-D1) is that the silicon atoms in T4 and T4 sites are replaced by aluminum atoms, the other (Period-Mor-D2) is that the silicon atoms in T4 and T2 sites are substituted (see Scheme 2c for the position of aluminum atoms). There are two possible structures in site E, and both of them (Period-Mor-E1 (see Scheme 4a for the position of aluminum atoms) and Period-Mor-E2 (see Scheme 4b for the position of aluminum atom)) were calculated.

Cluster calculations have been performed with *Gaussian03*[40] using the 6-31g++** basis set[41] and DFT B3LYP method.[42−44] For zeolitic systems, this method has been shown to give properties comparable to MP2 calculations.[45,46] The basis set

SCHEME 2: Structures of Mg Cation Exchanged Mordenite Simulated with Cluster Approach after the Full Relaxation[a]

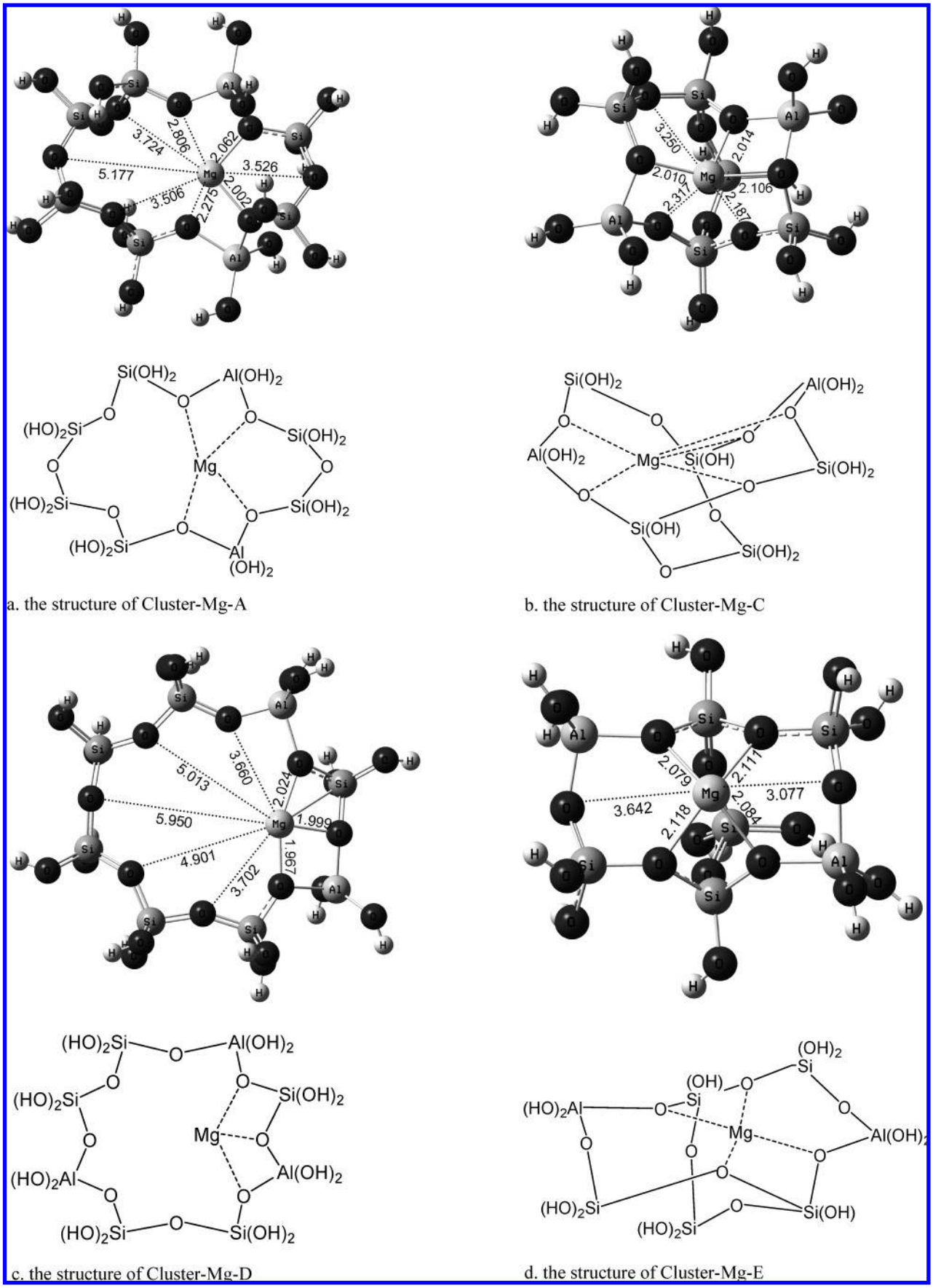

a. the structure of Cluster-Mg-A

b. the structure of Cluster-Mg-C

c. the structure of Cluster-Mg-D

d. the structure of Cluster-Mg-E

[a] The ball−stick models are the cluster models after relaxation. The numbers in the ball−stick models are the distances between oxygen atom and the Mg ion in angstroms.

TABLE 1: Total Energies for the Model Structure of Mg^{2+} Exchanged Mordenite Computed with the Periodic Approach

structures[a]	E (kJ mol^{-1})
*Period-Mor-A	−110494.1
Period-Mor-B1	−110349.9
Period-Mor-B2	−110405.4
*Period-Mor-C	−110505.8
Period-Mor-D1	−110343.5
*Period-Mor-D2	−110434.5
*Period-Mor-E1	−110446.8
Period-Mor-E2	−110435.2

[a] The asterisk means that the structure is more stable and is selected for the calculation with the cluster approach.

6-31g++** has been used for all atoms. Within the cluster approach, the catalytic active site model is a small neutral zeolite fragment, terminated with hydroxyl groups. The clusters were selected on the basis of the results of periodical simulation (vide post). Cluster-Mg-A [$MgO_8(Si_6Al_2)(OH)_{16}$] consists of a simple eight-ring to simulate the Mg cation in site A (see Scheme 2a). Cluster-Mg-C [$MgO_8(Si_5Al_2)(OH)_{12}$] is a six-ring with an additional O−T−O bridge for Mg located in site C (see Scheme 2b). Cluster-Mg-D [$MgO_8(Si_6Al_2)(OH)_{16}$] consists of an eight-ring to simulate the Mg cation in site D (see Scheme 2c). Cluster-Mg-E [$MgO_8(Si_5Al_2)(OH)_{12}$] is a six-ring with an additional O−T−O bridge for Mg^{2+} located in site E (see Scheme 2d).

Partial geometry optimizations of these cluster compounds were performed, in which the position of all atoms was optimized, except for the dangling OH bonds. For the latter, the position of oxygen atoms was fixed. Geometry optimization calculations were carried out to obtain a local minimum energy for zeolite fragment and adsorption complexes. The frequencies of adsorbed CO were computed using analytical second derivatives and were scaled by 0.9613.[47]

Experimental Details. MgK-mordenite (Mg and K exchanged mordenite) sample was prepared by the ion exchange of sodium-mordenite. Sodium in Na-mordenite was exchanged for three times using an excess of 0.5 mol/L KCl solution stirred at 323 K for 12 h. Then the potassium of the sample was exchanged for three times with 0.5 mol/L $MgCl_2$ solution at 323 K for 12 h. The solid product was filtered, washed thoroughly with distilled water, dried overnight in an oven at 393 K.

IR spectra of adsorbed CO were recorded on a FT-IR spectrometer (Impact 410, Nicolet) equipped with a DTGS detector at a resolution of 4 cm^{-1} and at a typical averaging of 64 scans. Pretreatment of freshly prepared disks was carried out as follows: the sample was heated to 723 K in air and then evacuated at 723 K for 120 min. The IR spectrum of the bare pretreated disk recorded at room temperature was used as the background spectrum. CO (2.7×10^3 Pa at equilibrium) gas was introduced into the cell at room temperature. The IR spectra of the CO adsorbed sample were recorded at different temperatures (183−378 K) after the adsorption equilibrium was reached. The spectra of the ν(CO) region were obtained as the difference spectra by subtracting the background spectrum from the original spectra.

Results and Discussion

IR Spectra of Adsorbed CO on MgK-Mordenite. Figure 1a shows the IR spectra of adsorbed CO to a MgK-mordenite sample as a function of increasing temperature. At lower temperatures (*e.g.*, 183 K), five IR bands are observed at 2220, 2200, 2177, 2162 and 2137 cm^{-1}. The band at 2137 cm^{-1} is readily assigned to physically adsorbed CO inside the zeolite channels.[48] The band at 2162 cm^{-1} is assigned to the adsorbed CO polarized by K^+ cations located in the main channels.[48] The bands at 2220, 2200 and 2177 cm^{-1} are assigned to adsorbed CO on Mg^{2+} cations in the channels of mordenite.

Figure 1a also shows that the band intensity at 2177 cm^{-1} is decreased most rapidly among the three bands at 2220, 2200 and 2177 cm^{-1} with the increasing temperature. Subsequently the band at 2200 cm^{-1} decreases in intensity more rapidly than the band at 2220 cm^{-1} but slower than the band at 2177 cm^{-1}. This indicates that the adsorption energies of CO adsorbed on Mg^{2+} cations at different sites are different, and the sequence of the adsorption energies corresponding to the vibrational frequencies of adsorbed CO is as follows: 2177 cm^{-1} < 2200 cm^{-1} < 2220 cm^{-1}. At low temperatures (*e.g.*, 183 K), the IR intensity follows the sequence 2177 cm^{-1} > 2200 cm^{-1} > 2220 cm^{-1}. This suggests that the sequence of the amounts of Mg^{2+} cations at different sites is the site corresponding to 2177 cm^{-1} > 2200 cm^{-1} > 2220 cm^{-1}.

SCHEME 3: Final Structure of Mordenite with Exchanged Mg^{2+} at Initial Site B2 (Period-Mor-B2)

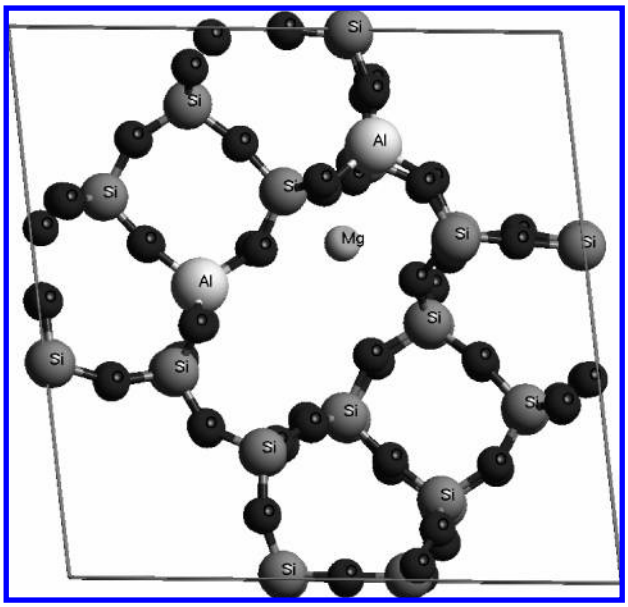

SCHEME 4: Location of Al Atoms in the Structures of Period-Mor-E1 (a) and Period-Mor-E2 (b)

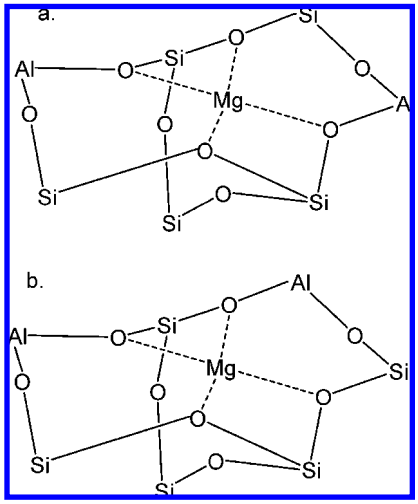

TABLE 2: Calculated and Experimental IR Frequencies (ω_{CO}) of Adsorbed CO and Frequency Shifts ($\Delta\omega$) of Adsorbed CO on Mg/Mordenite[a]

	sites	ω_{CO} (exp)	$\Delta\omega$ (exp)	ω_{CO} (periodic)	$\Delta\omega$ (periodic)	ω_{CO} (cluster)	$\Delta\omega$ (cluster)	intensity ω_{CO} (cluster)
main channel	E	2220	77	2157.9	77.7	2210.3	93.2	56.4
	D	2220	77	2151.7	71.5	2214.4	97.3	36.6
side channel	A	2200	57	2146.9	66.7	2199.3	82.2	51.1
side pocket	C	2177	34	2118.4	38.2	2177.0	59.9	89.2
free CO		2143	0	2080.2	0.0	2117.1	0.0	86.5

[a] "Periodic" means that the results were obtained with periodical approach, and "cluster" means that the results were obtained with the cluster approach; "exp" means the experimental results. The units are cm^{-1}.

The sites in the side pockets (site C) or in the side channels (site A and site B) are more shielded by framework oxygen ions (negatively charged) and therefore exert a smaller polarization on adsorbed CO molecules. This is reflected in a smaller blue shift of the C−O stretching vibration than those of CO on sites in the main channels (site D and site E).[49] Therefore, the band at 2220 cm^{-1} is assigned to the adsorbed CO on Mg^{2+} ions located in the main channels (site D or site E). The bands at 2200 and 2177 cm^{-1} are assigned to the adsorbed CO polarized by Mg^{2+} ions located in the side pockets (site C) or the side channels (site A or site B). However, the bands between 2200 and 2177 cm^{-1} could be for CO adsorbed either on the sites in the side pockets (site C) or on the sites in the side channels (site A or site B) only from IR results.

Stability of Mg^{2+} at Different Sites in Mg-Mordenite Calculated by Periodical Calculations. The models of Mg^{2+} exchanged mordenite (Mg-MOR) have been optimized within the ultrasoft pseudopotentials (USPP) potentials and the calculated total energies of these structures are listed in Table 1. Comparing the total energies of the structures of Mg^{2+} in Mg-MOR at different sites, the sequence of stability of Mg^{2+} ions in Mg-MOR is site C > site A > site E1 > site E2 > site D2 > site B2 > site B1 > site D1. The structures of Period-Mor-B1 and Period-Mor-D1 are not possibly presence, because their energies are much higher (more than 80 kJ mol^{-1}) than those of the stable structures.

The energy of Period-Mor-B2 is 30 kJ mol^{-1} higher than those of the stable strucutures, so the structure of Period-Mor-B2 is unstable. Furthermore, from simulated results, the Mg^{2+} cation is initially in site B2 but moves into site A after a full structural relaxation (see Scheme 3 for the final structure). According to the experimental results,[9] site A is occupied by ions with a radius smaller than 1.3 Å and site B by ions with a radius larger than 1.3 Å. Because a Mg^{2+} cation with a radius of 0.66 Å should prefer site A, it will not occupy site B. Therefore, the Mg^{2+} cations exist in sites A, C, D and E and the predicted stability sequence of Mg^{2+} ions in these sites is site C > site A > site E > site D. This is in good agreement with the simulations using force fields.[50]

For Mg^{2+} cations in site E, the energy of Period-Mor-E1, with the structure of both aluminums in opposite positions (see Scheme 4a) is 11.6 kJ mol^{-1} lower than that of Period-Mor-E2, with the structure of both aluminums in same side (see Scheme 4b). It shows that the structure with two aluminums in opposite positions in site E is a more stable structure. A calculation on Cu^{2+} in mordenite also indicated that Cu/Mor-E1 (both aluminums in opposite positions) is 8.4 kJ mol^{-1} lower than that of Cu/Mor-E2 (both aluminums in parallel positions).[39] Therefore, the structure of Mor-E1 with both aluminums in opposite positions was chosen as a model to study the surrounding of site E. The most stable structures from the periodical calculations (Period-Mor-A, Period-Mor-C, Period-Mor-D2, Period-Mor-E1) are selected for further DFT calculations.

Calculated IR Frequencies of CO Adsorbed on Mg-Mordenite. Table 2 shows that the blue shift of the stretching frequencies of adsorbed CO on sites A, C, D and E simulated with the periodical approach are 66.7, 38.2, 71.5 and 77.7 cm^{-1} respectively, whereas the cluster simulation results are 82.2, 59.9, 97.3 and 93.2 cm^{-1}, respectively. Both results show that the blue shift of adsorbed CO on Mg cation in site C is the smallest and that in site A is the second smallest. This is supported by the truth that the sites in the narrower channels (site A and site C) are more shielded by framework oxygen ions and therefore induce a smaller blue shift of the C−O strectching vibration than those on the sites in the broader channels (sites D and E).[49] It suggests that the band with the lowest frequency (2177 cm^{-1}) in IR spectra should be assigned to CO adsorbed on Mg cations in site C and the band at 2200 cm^{-1} should be assigned to CO adsorbed on Mg cations in site A.

The cluster results show that the blue shift of adsorbed CO on Mg cations in site D is the largest; however, the largest blue shift by periodical approach is predicted in site E. It seems that they conflict with each other. Actually, the predicted frequency difference between adsorbed CO on Mg cations in site D and site E is only several wavenumbers no matter by cluster approach or periodical approach. This difference with several wavenumbers is so small that it is almost in the range of computational error bar. Therefore, it is concluded that the band at 2220 cm^{-1} in IR spectra is essentially due to a mixture of the bands of adsorbed CO on Mg^{2+} in sites E and D. Furthermore, the band at 2200 cm^{-1} is to be assigned to the CO adsorbed on a Mg^{2+} cation in the side pockets (site C). The band at 2177 cm^{-1} is assigned to the CO adsorbed on a Mg^{2+} cation in the side channels (site A) (see Figure 1a). Because the magnitude of the blue shift of adsorbed CO measures the corresponding electrostatic field strength surrounding the active centers, the sequence of electrostatic field strength surrounding the Mg cation in different sites should be in the following order: site D, site E > site A > site C.

It is noticed that the calculated IR intensity of a CO molecule adsorbed to a Mg cation at different sites varies from 36.6 to 89.2 (see Table 2). Therefore, the IR intensity of the band of saturated adsorbed CO at low temperature can reflect an approximate distribution of different sites in the zeolite. The relative distribution of Mg^{2+} cations in mordenite at different sites from IR spectroscopy is, site C > site A > site D and site E. This agrees with the calculated stability of Mg^{2+} at different sites in Mg-mordenite by periodical simulation.

Adsorption Energies of CO on Mg-Mordenite. Table 3 gives the adsorption energies of CO adsorbed on Mg cation at different site in mordenite estimated from the periodic structure models. It shows that the sequence of adsorption energies of CO on Mg-mordenite deduced from the periodical approach is, site D, site E > site A > site C. Because the vibrational frequencies of adsorbed CO on site D and site E are indistinguishable by IR spectroscopy, the calculated preferable adsorp-

TABLE 3: Adsorption Energies of CO Adsorbed on Mg-Mordenite Calculated by Periodical DFT Simulation

structures	$E_{adsorption}$ (kJ mol^{-1})
Period-Mor-A	−65.0
Period-Mor-C	−49.7
Period-Mor-D	−95.6
Period-Mor-E	−90.7

tion energy sequence of adsorbed CO on Mg^{2+} is site D and site E (at 2220 cm^{-1}), site A (at 2200 cm^{-1}) and site C (at 2177 cm^{-1}). The experimental results give the same sequence (see Figure 1a).

Because cluster models using a discrete basis set and different exchange functional are suitable to computing vibrational frequencies,[18−24] the absolute values of frequencies computed from cluster models will be best compared with the experimental results. According to the calculated vibrational frequencies by cluster approach and the calculated stability of Mg^{2+} at different sites and calculated adsorption energies of adsorbed CO on Mg cations by periodical simulation, a scheme of calculated IR spectra of adsorbed CO on Mg/mordenite with the increasing temperature was drawn in Figure 1b. The good agreement of between Figure 1a and Figure 1b suggests that the assignment of these bands of adsorbed CO is reasonable.

The absolute adsorption energies of CO adsorbed in sites D, E, A and C on Mg-mordenite according to the periodical approach are −95.6, −90.7, −65.0 and −49.7 kJ mol^{-1}, respectively. The experimental adsorption energy of CO on Mg-mordenite is about −66.1 kJ mol^{-1},[51] so the periodical simulations are in good agreement with the experimental results.

From the calculated stability of Mg^{2+} cation at different sites in the channels of mordenite, it could be estimated that the Mg^{2+} cation in site D and site E with the highest blue shift of adsorbed CO has the lowest concentration and the highest binding energy of adsorbed CO. The highest probability of Mg^{2+} cation adsorption appears to be site C. Both the blue shift of adsorbed CO and binding energy between Mg^{2+} and adsorbed CO are the lowest. This is supported by the IR spectra of adsorbed CO on MgK-mordenite (Figure 1a).

For an exchanged cation at a site in the channel of zeolite, the framework can strongly interact with the cation if the surrounding of the site (*e.g.*, in narrow channels) has strong electrostatic shield. Therefore, the cation with strong interaction in the site is stable. The cation in such stable site is more shielding than that in an unstable site, and the more shielding cation has the weaker electrostatic field. Because the electrostatic field of the cation is directly related to the frequency of adsorbed CO, the adsorbed CO on the more shielding cation has a lower frequency. The more shielding cation has weaker interaction with the adsorbed CO, because the cation in stable site is stable alone. In general, the cation in the stable site with the high concentration has the weak electrostatic field strength, and the frequency and the adsorption energy of the adsorbed CO on the cation is low.

Conclusions

From the study of IR spectra of the adsorbed CO on MgK-mordenite, there are at least three kinds of sites in mordenite that can be occupied by Mg cations. The IR bands of CO adsorbed on Mg^{2+} located in these sites are 2177, 2200 and 2220 cm^{-1}. The sequence of the adsorption energies corresponding to the vibrational frequencies of adsorbed CO is 2177 cm^{-1} < 2200 cm^{-1} < 2220 cm^{-1}. The sequence of stability of Mg^{2+} cations at different sites in mordenite characterized by the IR bands of adsorbed CO is 2177 cm^{-1} > 2200 cm^{-1} > 2220 cm^{-1}, respectively.

By combining DFT simulations and IR spectroscopy, we can assign the band at 2220 cm^{-1} to CO adsorbed on Mg^{2+} cations in sites E and D in the main channels. The Mg^{2+} cations in sites E and D in the mordenite have the lowest concentration and the strongest interaction with CO. The band at 2200 cm^{-1} is assigned to the CO adsorbed on the Mg^{2+} cation in site A in the side channels, and the interaction between adsorbed CO and Mg^{2+} cation in site A is moderate. The band at 2177 cm^{-1} is assigned to CO adsorbed on the Mg^{2+} cation in site C in the side pockets, and the Mg^{2+} in site C has the highest concentration and the weakest interaction with CO. The combination of the DFT simulations and IR spectroscopy has been demonstrated to be able to identify the exchanged cations in zeolites and to characterize the properties of molecular adsorption on the cation sites in zeolites.

Acknowledgment. We are grateful to Programme for Strategic Scientific Alliances between the China and The Netherlands (PSA), Royal Netherlands Academy of Arts and Sciences (KNAW) (Grant No. 04-PSA-M-01) and National Basic Research Program of China (Grant No. 2004CB720607) for financial support. We are also grateful to 973 Project (Grant No. 2003CB615806, No. 2005CB221407) and the Natural Science Foundation of China (NSFC Grant No. 20273069, NSFC Grant No. 20520130214, NSFC Grant No. 20673115).

References and Notes

(1) Moscou, L. In *Introduction to Zeolite Science and Practice*; Bekkum, H. V., Flanigen, E. M., Jansen, J. C., Eds.; Studies in Surface Science and Catalysis, vol. 58; Elsevier: Amsterdam, 1991; p 1.
(2) Stöcker, M. *Microporous Mesoporous Mater*. **1999**, *29*, 3.
(3) Froment, G. F.; Dehertog, W. J. H.; Marchi, A. J. *Catalysis* **1992**, *9*, 1.
(4) van Donk, S.; Broersma, A.; Gijzeman, O. L. J.; van Bokhoven, J. A.; Bitter, J. H.; de Jong, K. P. *J. Catal*. **2001**, *204*, 272.
(5) Feng, X. B.; Hall, W. K. *J. Catal*. **1997**, *166*, 368.
(6) Li, Y. J.; Armor, J. N. *J. Catal*. **1994**, *150*, 376.
(7) Wichterlová, B.; Dědeček, J.; Sobalík, Z.; Vondrová, A.; Klier, K. *J. Catal*. **1997**, *169*, 194.
(8) Dědeček, J.; Wichterlová, B. *J. Phys. Chem. B* **1999**, *103*, 1462.
(9) (a) Mortier, W. J.; Pluth, J. J.; Smith, J. V. *Mater. Res. Bull*. **1975**, *10*, 1037. (b) Mortier, W. J. *J. Phys. Chem*. **1977**, *81*, 1334. (c) Schlenker, J. L.; Pluth, J. J.; Smith, J. V. *Mater. Res. Bull*. **1979**, *14*, 961.
(10) Dědeček, J.; Sobalík, Z.; Tvarůžková, Z.; Kaucký, D.; Wichterlová, B. *J. Phys. Chem.* **1995**, *99*, 16327.
(11) Sobalík, Z.; Tvarůžková, Z.; Wichterlová, B. *J. Phys. Chem. B* **1998**, *102*, 1077.
(12) Giamello, E.; Murphy, D.; Magnacca, G.; Morterra, C.; Shioya, Y.; Nomura, T.; Anpo, M. *J. Catal*. **1992**, *136*, 510.
(13) Scarano, D.; Spoto, G.; Bordiga, S.; Coluccia, S.; Zecchina, A. *J. Chem. Soc., Faraday Trans*. **1992**, *88*, 291.
(14) Nachtigallová, D.; Bludský, O.; Otero Areán, C.; Bulánek, R.; Nachtigall, P. *Phys. Chem. Chem. Phys*. **2006**, *8*, 4849.
(15) Garrone, E.; Bulánek, R.; Frolich, K.; Otero Areán, C.; Rodríguez Delgado, M.; Palomino, G. T.; Nachtigallová, D.; Nachtigall, P. *J. Phys. Chem. B* **2006**, *110*, 22542.
(16) Benco, L.; Bucko, T.; Hafner, J.; Toulhoat, H. *J. Phys. Chem. B* **2004**, *108*, 13656.
(17) Bučko, T.; Hafner, J.; Benco, L. *J. Phys. Chem. B* **2005**, *109*, 7345.
(18) Del Vitto, A.; Giordano, L.; Pacchioni, G.; Heiz, U. *J. Phys. Chem. B* **2005**, *109*, 3416.
(19) García-Hernández, M.; López, N.; Moreira, I. de P. R.; Paniagua, J. C.; Illas, F. *Surf. Sci.* **1999**, *430*, 18.
(20) Widjaja, Y.; Musgrave, C. B. *Surf. Sci*. **2000**, *469*, 9.
(21) Giordano, L.; Pacchioni, G.; Bredow, T.; Sanz, J. F. *Surf. Sci*. **2001**, *471*, 21.
(22) Rodriguez, J. A.; Ricart, J. M.; Clotet, A.; Illas, F. *J. Chem. Phys*. **2001**, *115*, 454.
(23) Fielicke, A.; von Helden, G.; Meijer, G.; Pedersen, D. B.; Simard, B.; Rayner, D. M. *J. Phys. Chem. B* **2004**, *108*, 14591.
(24) Wang, G. C.; Jiang, L.; Morikawa, Y.; Nakamura, J.; Cai, Z. S.; Pan, Y. M.; Zhao, X. Z. *Surf. Sci*. **2004**, *570*, 205.

(25) Sun, H.; Blatter, F.; Frei, H. *J. Am. Chem. Soc.* **1994**, *116*, 7951.
(26) Sun, H.; Blatter, F.; Frei, H. *J. Am. Chem. Soc.* **1996**, *118*, 6873.
(27) Li, Y. G.; Xie, W. H.; Yong, S. *Appl. Catal. A: General* **1997**, *150*, 231.
(28) Hadjiivanov, K.; Ivanova, E.; Knözinger, H. *Microporous Mesoporous Mater.* **2003**, *58*, 225.
(29) (a) Kresse, G.; Hafner, J. *Phys. Rev. B* **1993**, *48*, 13115. (b) Kresse, G.; Hafner, J. *Phys. Rev. B* **1994**, *49*, 14251. (c) Kresse, G.; Furthmüller, J. *Comput. Mater. Sci.* **1996**, *6*, 15. (d) Kresse, G.; Furthmüller, J. *Phys. Rev. B* **1996**, *54*, 11169.
(30) Perdew, J. P.; Zunger, A. *Phys. Rev. B* **1981**, *23*, 5048.
(31) Perdew, J. P.; Burke, K.; Wang, Y. *Phys. Rev. B* **1996**, *54*, 16533.
(32) Kresse, G.; Hafner, J. *J. Phys. Condens. Matter.* **1994**, *6*, 8245.
(33) Demuth, T.; Hafner, J.; Benco, L.; Toulhoat, H. *J. Phys. Chem. B* **2000**, *104*, 4593.
(34) Simoncic, P.; Armbruster, T. *Am. Miner.* **2004**, *89*, 421.
(35) Mortier, W. *Compilation of Extra Framework Sites in Zeolites*; Butterworths Sci. Ltd.: Guilord, 1982.
(36) Loewenstein, W. *Am. Miner.* **1954**, *39*, 92.
(37) Takaishi, T.; Kato, M.; Itabashi, K. *Zeolites* **1995**, *15*, 21.
(38) Takaishi, T.; Kato, M.; Itabashi, K. *J. Phys. Chem.* **1994**, *98*, 5742.
(39) Delabie, A.; Pierloot, K.; Groothaert, M. H.; Weckhuysen, B. M.; Schoonheydt, R. A. *Phys. Chem. Chem. Phys.* **2002**, *4*, 134.
(40) Frisch, M. J.; Trucks, G. W.; Schlegel, H. B.; Scuseria, G. E.; Robb, M. A.; Cheeseman, J. R.; Montgomery, J. A., Jr.; Vreven, T.; Kudin, K. N.; Burant, J. C.; Millam, J. M.; Iyengar, S. S.; Tomasi, J.; Barone, V.; Mennucci, B.; Cossi, M.; Scalmani, G.; Rega, N.; Petersson, G. A.; Nakatsuji, H.; Hada, M.; Ehara, M.; Toyota, K.; Fukuda, R.; Hasegawa, J.; Ishida, M.; Nakajima, T.; Honda, Y.; Kitao, O.; Nakai, H.; Klene, M.; Li, X.; Knox, J. E.; Hratchian, H. P.; Cross, J. B.; Adamo, C.; Jaramillo, J.; Gomperts, R.; Stratmann, R. E.; Yazyev, O.; Austin, A. J.; Cammi, R.; Pomelli, C.; Ochterski, J. W.; Ayala, P. Y.; Morokuma, K.; Voth, G. A.; Salvador, P.; Dannenberg, J. J.; Zakrzewski, V. G.; Dapprich, S.; Daniels, A. D.; Strain, M. C.; Farkas, O.; Malick, D. K.; Rabuck, A. D.; Raghavachari, K.; Foresman, J. B.; Ortiz, J. V.; Cui, Q.; Baboul, A. G.; Clifford, S.; Cioslowski, J.; Stefanov, B. B.; Liu, G.; Liashenko, A.; Piskorz, P.; Komaromi, I.; Martin, R. L.; Fox, D. J.; Keith, T.; Al-Laham, M. A.; Peng, C. Y.; Nanayakkara, A.; Challacombe, M.; Gill, P. M. W.; Johnson, B.; Chen, W.; Wong, M. W.; Gonzalez, C.; Pople, J. A. *Gaussian03*; Gaussian, Inc.: Pittsburgh, PA, 2003.
(41) (a) Petersson, G. A.; Al-Laham, M. A. *J. Chem. Phys.* **1991**, *94*, 6081. (b) Petersson, G. A.; Bennett, A.; Tensfeldt, T. G.; Al-Laham, M. A.; Shirley, W. A.; Mantzaris, J. *J. Chem. Phys.* **1988**, *89*, 2193.
(42) Beche, A. D. *Phys. Rev. A* **1988**, *38*, 3098.
(43) Lee, C.; Yang, W.; Parr, R. G. *Phys. Rev. B* **1988**, *37*, 785.
(44) Beche, A. D. *J. Chem. Phys.* **1993**, *98*, 5648.
(45) Civalleri, B.; Garrone, E.; Ugliengo, P. *J. Phys. Chem. B* **1998**, *102*, 2373.
(46) Zygmunt, S. A.; Mueller, R. M.; Curtiss, L. A.; Iton, L. E. *J. Mol. Struct.* **1998**, *430*, 9.
(47) Foresman, J. B.; Frisch, Æ. *Exploring Chemistry with Electronic Structure Methods*; 2nd ed.; Gaussian, Inc.: Carnegie Office Park, Building 6, Pittsburgh, PA, 1996; pp 64.
(48) Bordiga, S.; Lamberti, C.; Geobaldo, F.; Zecchina, A.; Palomino, G. T.; Areán, C. O. *Langmuir* **1995**, *11*, 527.
(49) Pidko, E. A.; Xu, J.; Mojet, B. L.; Lefferts, L.; Subbotina, I. R.; Kazansky, V. B.; van Santen, R. A. *J. Phys. Chem. B* **2006**, *110*, 22618.
(50) Maurin, G.; Bell, R. G.; Devautour, S.; Henn, F.; Giuntini, J. C. *Phys. Chem. Chem. Phys.* **2004**, *6*, 182.
(51) Furuyama, S.; Nagato, M. *J. Phys. Chem.* **1984**, *88*, 1735.